

A Set of Ground Penetrating Radar Measures from Quarries

Stefano Bonduà ^{1,*} , André Monteiro Klen ², Massimiliano Pilone ³, Laurentiu Asimopolos ⁴ 
and Natalia-Silvia Asimopolos ⁴ 

¹ DICAM—Alma Mater Studiourum, University of Bologna, 40131 Bologna, Italy

² Federal Institute of Education, Science and Technology of Minas Gerais, Ouro Preto 35400-000, Brazil; andre.klen@ifmg.edu.br

³ Geologist Massimiliano Pilone, 65122 Pescara, Italy; pilonemassimiliano@gmail.com

⁴ Geological Institute of Romania, 012271 Bucharest, Romania; laurentiu.asimopolos@igr.ro (L.A.); natalia.asimopolos@igr.ro (N.-S.A.)

* Correspondence: stefano.bondua@unibo.it

Abstract: This paper presents a set of Ground Penetrating Radar (GPR) data obtained from in situ measurements conducted in four ornamental stone quarries located in Italy (Botticino quarry) and Romania (Ruschita, Carpinis, and Pietroasa quarries). The GPR is a Non-Destructive Testing (NDT) technique that enables the detection and localization of fractures without damage to the surface, among other capabilities. In this study, two instruments of ground-coupled GPR were used to detect and locate the fractures, discontinuities, or weakened zones. The GPR data contains radargrams for discontinuities and fracture detection, besides the geographic location of the measures. For each measurement site, a set of radargrams has been acquired in two orthogonal directions, allowing for a 3D reconstruction of the investigated site.

Dataset: DOI:10.17632/w26n6nftxs.3 (<https://data.mendeley.com/datasets/w26n6nftxs/3>)

Dataset License: CC BY-NC-ND

Keywords: fracture detection; ground penetrating radar (GPR); non-destructive testing (NDT); quarries; ornamental stones



Citation: Bonduà, S.; Monteiro Klen, A.; Pilone, M.; Asimopolos, L.; Asimopolos, N.-S. A Set of Ground Penetrating Radar Measures from Quarries. *Data* **2024**, *9*, 42. <https://doi.org/10.3390/data9030042>

Received: 22 September 2023

Revised: 19 December 2023

Accepted: 23 February 2024

Published: 3 March 2024



Copyright: © 2024 by the authors. Licensee MDPI, Basel, Switzerland. This article is an open access article distributed under the terms and conditions of the Creative Commons Attribution (CC BY) license (<https://creativecommons.org/licenses/by/4.0/>).

1. Summary

Upon the ERAMIN3 call, the project Artificial Intelligence Characterization Ornamental Stones Quarry Optimization (AI-COSTSQQO) started in April 2022. The AI-COSTSQQO project is focused on, among others, the detection and characterization of discontinuities and fractures of the rock mass, affecting ornamental stone production and, consequently, the generation of waste. Previous work in the scientific literature related to fracture detection based on Ground Penetrating Radar (GPR) measurement can be found in [1–11]. The fracture characterization allowed the development and use of optimization algorithms that can reduce the generation of waste for environmental protection, increase economic revenue, and increase the recovery ratio of the quarries. Among them, it is worth mentioning [12–17]. Previous work on GPR data can be found, among others, in [18–27].

This paper presents two GPR datasets. The first data set is related to an in-field investigation in Italy in a marble quarry. The second data set is related to marble quarries in Romania.

2. Site Description

2.1. Botticino Quarry (Italy)

The site of investigation is located in Botticino (Italy). The position of the Botticino Quarry in Google Earth Pro is 45°33′5.48″ N, 10°19′5.16″ E. The quarry (Figure 1) extracts

Botticino Classico marble. The Botticino Classico marble is exploited from the top layer of Corna's geologic formation, which is derived from carbonate mud sedimentation and rocks emerging from the marble basin.



Figure 1. Top view of the quarry located in Botticino (Google Earth Pro).

Their carbonate nature results from the diagenesis of marine deposits such as mud and organic and inorganic elements. Botticino Classico is the last remaining proof of the existence of a carbonate platform in Brescia. It is either found in solid form or in meters-long beds separated by clay joints.

Its lithology is mainly cementation of compact, lightly colored limestone, which varies in tone from white through to ivory with hints of chestnut. The rock has thin chestnut-colored stylolite, almost parallel to the sedimentation level.

Botticino Classico marble is an extremely compact carbonate rock; it has low water absorption and porosity levels and excellent mechanical qualities such as shock and wear resistance, even after undergoing a freezing–unfreezing cycle test. Strong, elegant, stunning in color, and easy to work, Botticino Classico is universally recognized as an excellent marble suitable for a wide variety of applications and internal and external use.

2.2. Ruschita Quarry (Romania)

Ruschita Quarry (Figure 2) is located in the northern part of Caras–Severin County, in Ruschita Village. The position of the Cava Ruschita Quarry in Google Earth Pro is $45^{\circ}38'46.03''$ N, $22^{\circ}24'24.83''$ E.



Figure 2. Top view of the Ruschita quarry (Google Earth Pro).

Ruschita marble is a metamorphic stone with high crystallinity and medium crystal size (up to 0.2–0.5 mm), with a compact structure and characteristic grain. Its basic color ranges from white and gray to pink, with many intermediate shades generally given by gray in the veins and less by impurities from the internal structure.

The stone shows irregular breakage, sometimes subsequent to very narrow internal discontinuities, invisible to macroscopic analysis. This material has superior physical and mechanical properties in terms of wear resistance and surface gloss. Mining methods consist of quarrying in horizontal benches (downwards) using diamond wire cutters, sewing machines (disks), and drilling and blasting technology.

2.3. Carpinis Quarry

Travertines are mined in the Carpinis Quarries and are the only resources of this type in Romania. Travertine is available in two shades: light brown and dark brown. It is exploited in an open quarry on the hills to the right of the Mures Valley, near Simeria Town, Carpinis Village, Hunedoara County.

The Carpinis quarry, owned by Marmosim SA, is situated in the Banpotoc–Carpinis travertine deposit within the southern chain of the Apuseni mountains, between the two places of the same name in the county of Hunedoara, about 4 km north of the town of Simeria and 1 km north of the Mures river. The position of the Carpinis Quarry (Figure 3) in Google Earth Pro is $45^{\circ}53'20.75''$ N, $23^{\circ}1'48.37''$ E.



Figure 3. Top view of the Carpinis quarry (Google Earth Pro).

The Carpinis travertine is found in the basement of the deposit, with intermediate thicknesses of 0–15 m. It is vesicular, sometimes breccia, friable, with greyish–yellowish and greyish–brownish spots, with clayey impurities and precipitations of SiO_2 . The Carpinis travertine gradually passes upwards into solid travertine, which is the best cultivable part. Massive travertine has a thickness of 2–40 m, small vacuoles, and a whitish–yellowish color.

The top of the sequence includes travertine slabs and clay deposits, representing the deposit cover with thicknesses of 1–15 m. The structure is microcrystalline, amorphous, or crustiform; the texture varies from vesicular to slightly vesicular to compact. There is usually a uniform distribution of vesicles in planes.

Under the microscope, different varieties of travertine have been distinguished: allochemical with aspartic cement, microsparitic and microsparitic with aragonitic cement, allochemical with micritic–sparitic cement, micritic–sparitic with bioclasts, and arenitic cement.

The deposit is affected by gravitational cracks, which can be open or poorly cemented by calcite or clay. The cracks are unevenly distributed but typically more than 2 m apart, affecting the size of the exploitation blocks to a lesser extent.

2.4. Pietroasa Quarry

The quarry is located in the hilly neighborhood of Deva Municipality, Hunedoara County, at an average altitude of +350 m. The position of the quarry (Figure 4) in Google Earth Pro is $45^{\circ}51'37.17''$ N, $22^{\circ}53'18.46''$ E. The stone produced by the quarry is the Pietroasa Andesite, which is a volcanic stone with a compact structure. It is very homogeneous, with a grey color and a uniform distribution of crystals, making it particularly suitable for outdoor applications.



Figure 4. Top view of the Pietroasa quarry (Google Earth Pro).

Pietroasa–Deva andesite is a variety of effusive magmatic rocks, named the andesite with hornblende from Pietroasa, which has a variegated appearance due to the mineralogical components. This stone exhibits excellent mechanical resistance and superior durability against atmospheric factors.

3. Data Description

The data presented in this work refer to an in situ investigation in quarries located in Italy and Romania using GPR instruments.

3.1. GPR Data: Italy

Instrument Description

The instrument employed in the Italian quarry was the Multifrequency Georadar Opera Duo, equipped with a single antenna but able to perform multi-frequency acquisition during a scan pass, with a frequency of 200 and 600 MHz, from IDS Georadar. This particular kind of GPR does not need calibration. The manufacturing date was 2021.

3.2. GPR Data: Romania

Instrument Description

The instrument used in the Romanian quarry was the Akula 9000C. It uses electromagnetic radiation in the microwave band (UHF/VHF frequencies; the range 10 MHz to 2.6 GHz) of the radio spectrum and detects the reflected signals from subsurface structures that can have applications in a variety of media, including rock, soil, and pavements. These signals are then digitally processed to create an image of the subsurface that can be used to identify discontinuities and other rock features using PRISM 2 software (version 2.70).

4. Data Acquisition

4.1. Italy's GPR Measure

The GPR measurement has been performed in three different locations near the working area (see Figure 5), and they are named grid 1, grid 2, and grid 3.

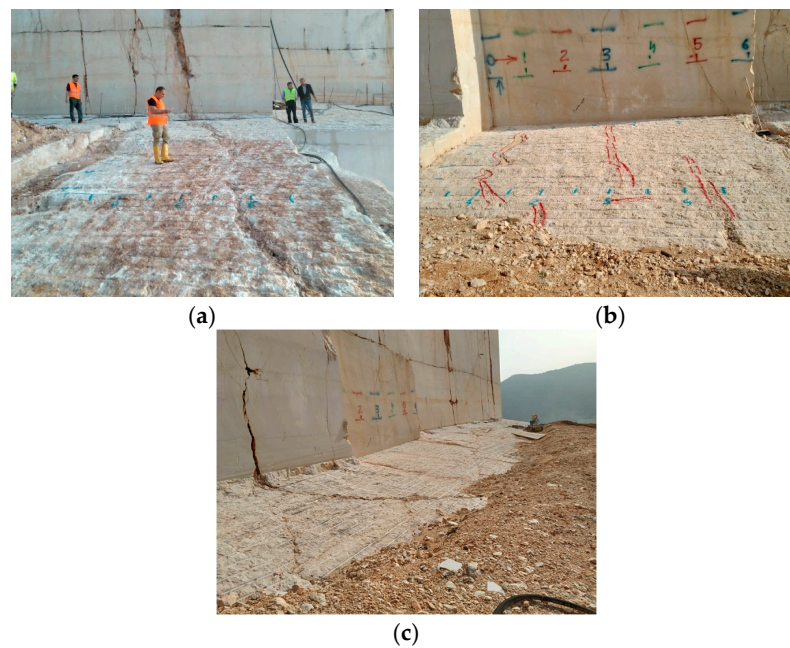


Figure 5. Botticino quarry. (a) Picture of grid 1; (b) Picture of grid 2; (c) Picture of grid 3. The fractures in the rock mass are clearly visible.

4.2. Grids Description

The grids have been created with a local coordinate system and geometry corresponding to a longitudinal and transversal pitch equal to 50 cm. They were defined on the basis of the roughness of the surface and the applicability of instrumental uses. Figure 6 shows a short description of the grids and naming convention for the scanlines.

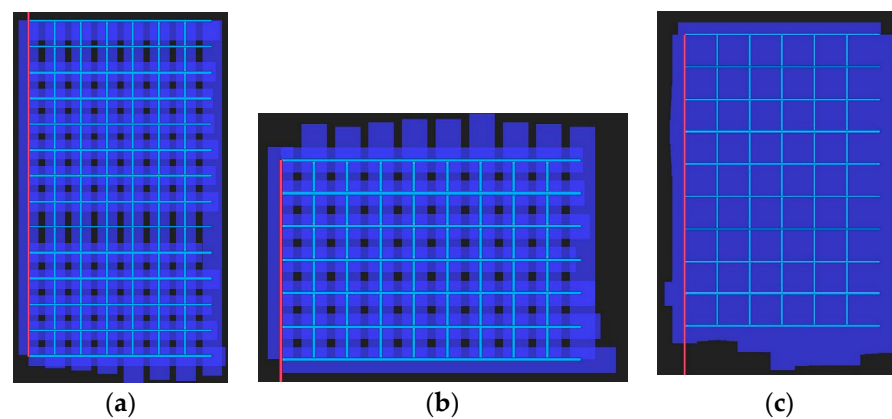


Figure 6. Schematic of the grids measure for the Marble quarry of Italy. (a) grid 1; (b) grid 2; (c) grid 3.

In order to scan the whole area of each location (grid 1, grid 2, and grid 3) and detect fractures or discontinuities, GPR scanlines were taken along the x-axis and parallel to the y-axis of local reference coordinate systems. Table 1 summarizes the information of the grids within the study area.

Table 1. GPR datasets collected within the study area.

Site	Number of Scan Lines	Scan Section (m × m)
Grid 1	8 × 14	3.5 × 6.5
Grid 2	10 × 7	4.5 × 3.5
Grid 3	7 × 10	3.5 × 5.5

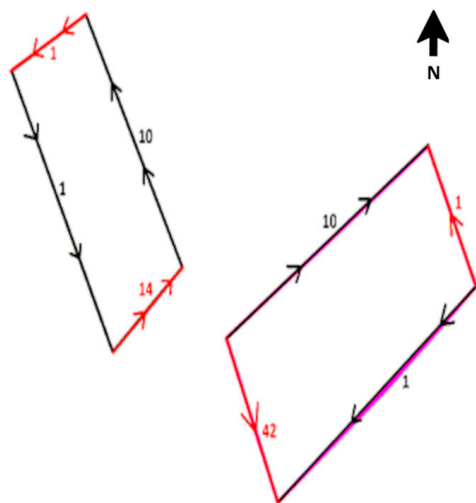
4.3. Romania GPR Measure

4.3.1. Ruschita Quarry

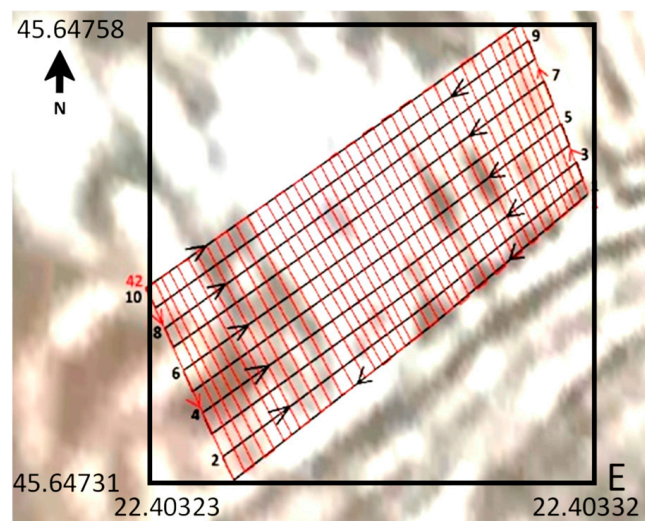
In the Ruschita quarry, two areas have been selected for the survey, and Figure 7 displays the schematic representation of the radargram acquisition map.



(a)



(b)



(c)

Figure 7. (a) Ruschita quarry; (b) Schematic map of the Ruschita quarry GPR survey. (c) Schematic profiles longitudinally and transversally of the Ruschita quarry GPR survey.

4.3.2. Carpinis Quarry

In the Carpinis quarry, due to the topography of the site, a narrow site area has been selected for the GPR Survey. Figure 8 shows the positions of the radargrams.

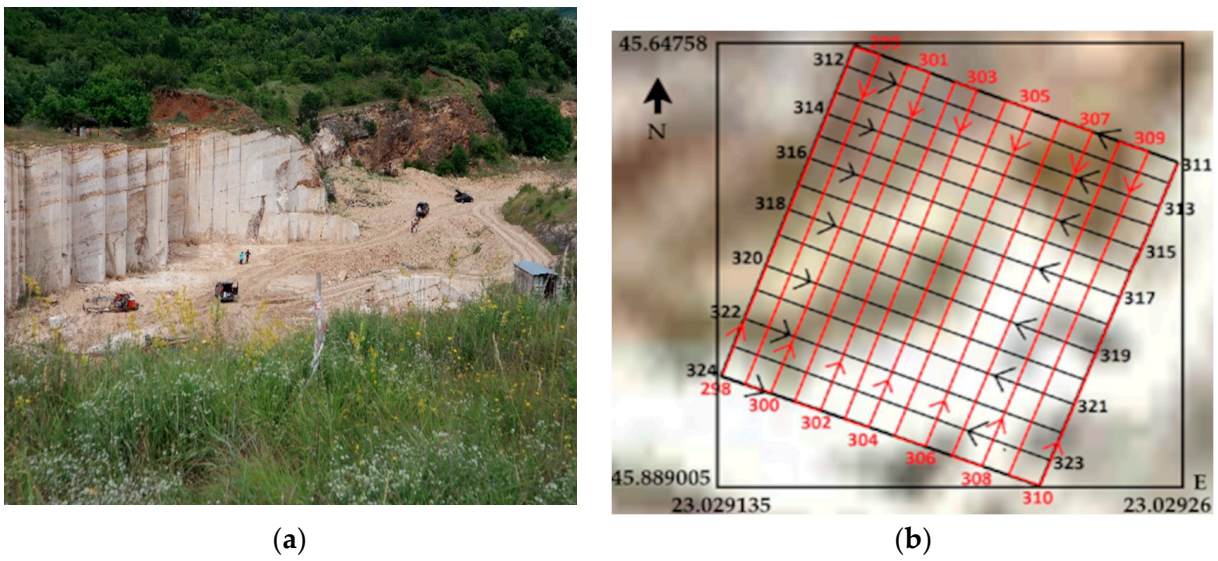


Figure 8. (a) Carpinis quarry; (b) Schematic map of the Carpinis quarry GPR survey.

4.3.3. Pietroasa Quarry

In the Pietroasa quarry, the surveyed area is shown in Figure 9.

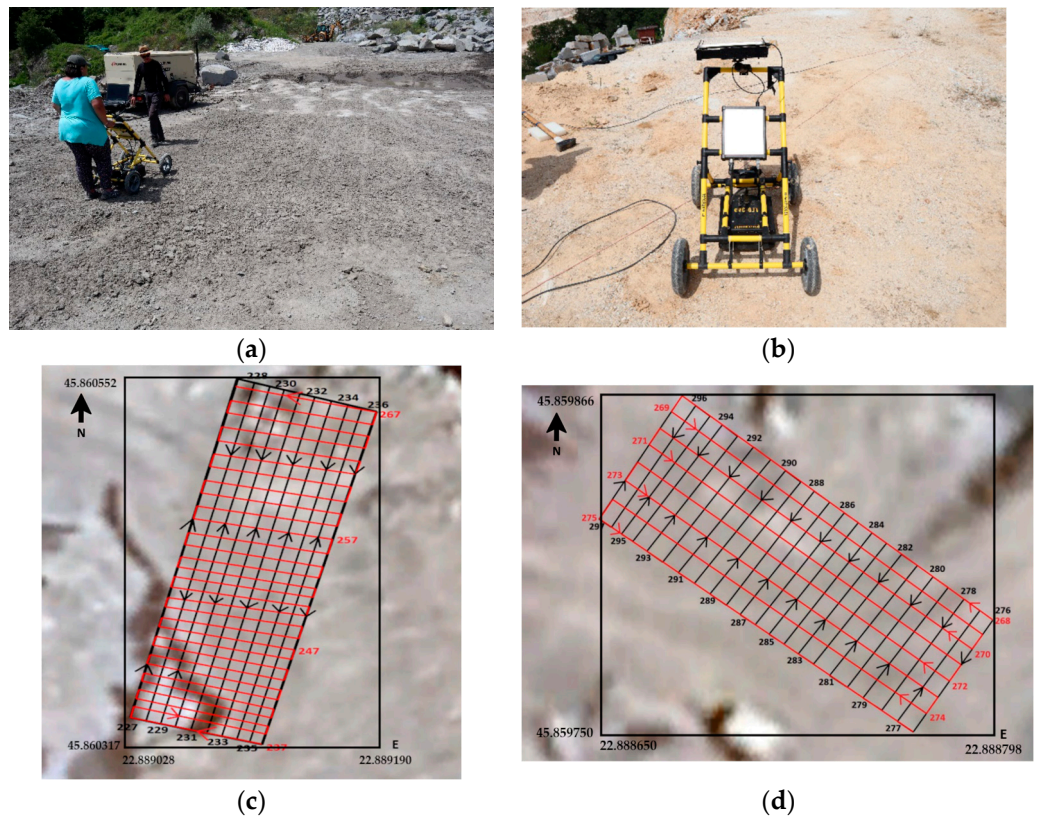


Figure 9. (a) In situ survey at Pietroasa quarry; (b) the Akulla 9000C unit; (c) Schematic map of the Pietroasa-1 down quarry GPR survey; (d) Schematic map of the Pietroasa 2 up quarry GPR survey.

5. Data Examples

5.1. Italy's GPR Data Example

The GPR survey in the three Italy locations allowed the radargram acquisition of each scanline. Figure 10 shows an example of a longitudinal radargram from grid 1 at a frequency of 200 MHz. Figure 10a is a radargram as acquired by the instrument without

digital filtering. Figure 10b presents the same radargram after filtering and noise removal. In this case, the propagation enables the analysis of the block up to a depth of approximately 430 cm.

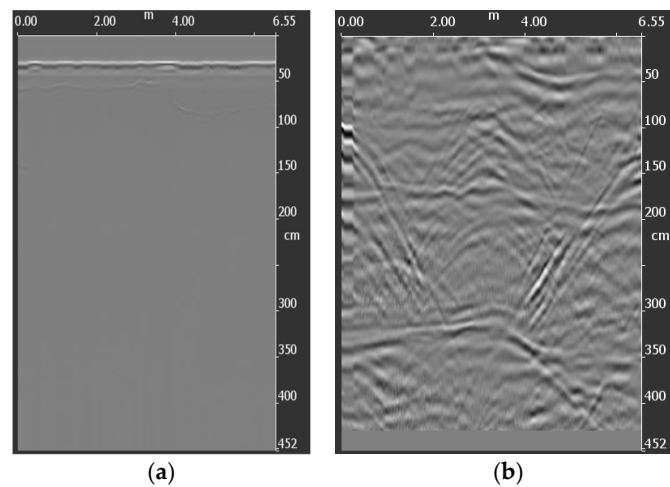


Figure 10. (a) Example of a raw radargram from grid 1; (b) Radargram after filtering and noise removal (filter applied: Band Pass in the time domain, 200–900 MHz, Soil Sample, Back Ground removal, signal gain of equalizer, with 1 m step application).

5.2. Romania's GPR Data Example

The GPR survey in the Romanian quarries allowed the radargram acquisition of each scanline.

Data examples of radargrams of only one profile from each quarry are presented for each quarry. In Figure 11 the radargram for Ruschita quarry, Figure 12 the radargram for Carpinis quarry, and Figure 13 the radargram for Pietroasa quarry. All the presented figures has been obtained from processing the GPR radargrams with the PRISM2 program.

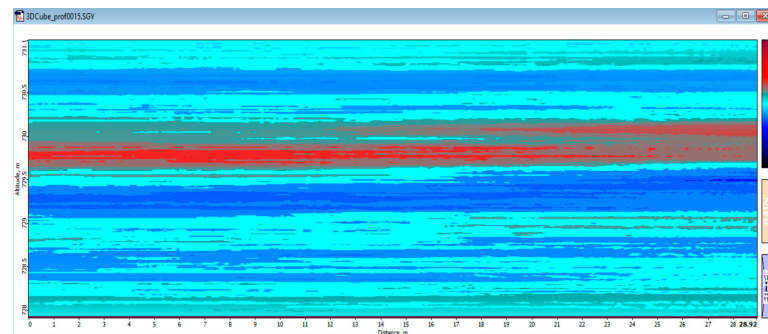


Figure 11. Radargram from Ruschita quarry.

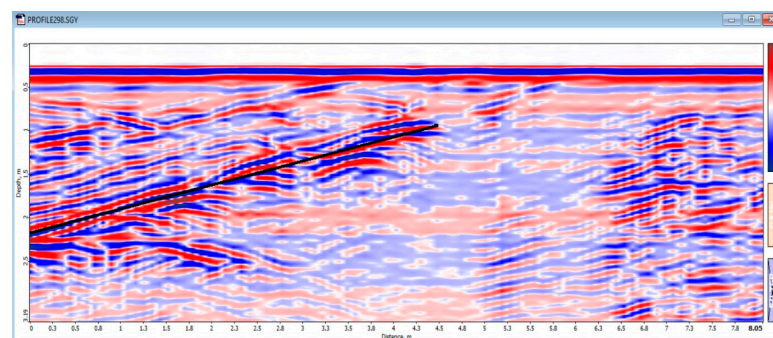


Figure 12. Radargram from Carpinis quarry.

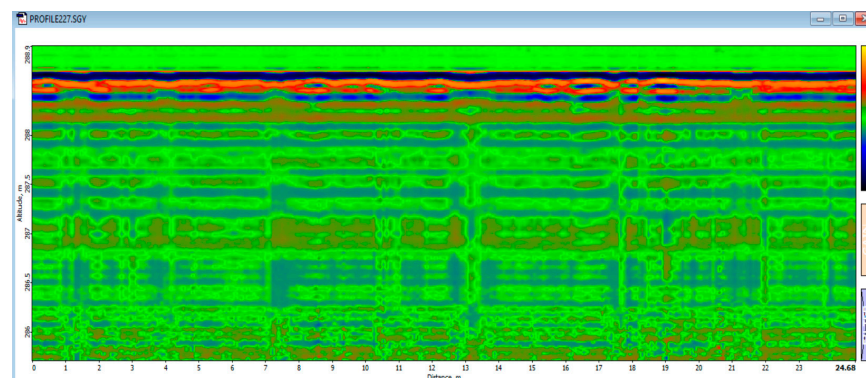


Figure 13. Radargram from Pietroasa quarry.

6. User Notes

This article introduces a novel dataset comprising GPR measurements conducted in marble quarries. These described datasets aim to provide researchers with opportunities for further exploration of GPR data for fracture detection. Additionally, they serve as valuable resources for educational purposes, implementing new algorithms, and establishing a reference for GPR measurements in ornamental stone quarries.

Author Contributions: Conceptualization, S.B., A.M.K., M.P., L.A., and N.-S.A.; methodology, S.B., A.M.K., M.P., L.A., and N.-S.A.; formal analysis, S.B., A.M.K., M.P., L.A., and N.-S.A.; investigation, S.B., A.M.K., M.P., L.A., and N.-S.A.; data curation, S.B., A.M.K., M.P., L.A., and N.-S.A.; writing—original draft preparation, S.B. and L.A.; writing—review and editing, S.B. and L.A.; supervision, S.B. and L.A.; project administration, S.B. and L.A.; funding acquisition, S.B. and L.A. All authors have read and agreed to the published version of the manuscript.

Funding: This research was funded by ERA-MIN, which has received funding from the European Union’s Horizon 2020 Research and Innovation Programme under grant agreements ERA-MIN 3. The APC was funded by the Italian Minister of Research MUR. Project title: AI-COSTSQO-Artificial Intelligence and Combined Survey Techniques for Stone Quarries Optimization, grant number: J35F21004410006.

Institutional Review Board Statement: Not applicable.

Informed Consent Statement: Not applicable.

Data Availability Statement: The data presented in this study are available at <https://data.mendeley.com/datasets/w26n6nftxs/3>.

Conflicts of Interest: The authors declare no conflicts of interest. The funders had no role in the design of the study, in the collection, analyses, or interpretation of data, in the writing of the manuscript, or in the decision to publish the results.

References

1. Theune, U.; Rokosh, D.; Sacchi, M.D.; Schmitt, D.R. Mapping fractures with GPR: A case study from Turtle Mountain. *Geophysics* **2006**, *71*, B139–B150. [[CrossRef](#)]
2. Dérobert, X.; Abraham, O. GPR and seismic imaging in a gypsum quarry. *J. Appl. Geophys.* **2000**, *45*, 157–169. [[CrossRef](#)]
3. Seol, S.J.; Kim, J.H.; Song, Y.; Chung, S.H. Finding the strike direction of fractures using GPR. *Geophys. Prospect.* **2001**, *49*, 300–308. [[CrossRef](#)]
4. Arosio, D. Rock fracture characterization with GPR by means of deterministic deconvolution. *J. Appl. Geophys.* **2016**, *126*, 27–34. [[CrossRef](#)]
5. Toshioka, T.; Tsuchida, T.; Sasahara, K. Application of GPR to detecting and mapping cracks in rock slopes. *J. Appl. Geophys.* **1995**, *33*, 119–124. [[CrossRef](#)]
6. Rey, J.; Martínez, J.; Montiel, V.; Cañadas, F.; Ruiz, N. Characterization of the sedimentary fabrics in ornamental rocks by using GPR. *Near Surf. Geophys.* **2017**, *15*, 457–465. [[CrossRef](#)]
7. Grandjean, G.; Gourry, J.C. GPR data processing for 3D fracture mapping in a marble quarry (Thassos, Greece). *J. Appl. Geophys.* **1996**, *36*, 19–30. [[CrossRef](#)]

8. Zanzi, L.; Hojat, A.; Ranjbar, H.; Karimi-Nasab, S.; Azadi, A.; Arosio, D. GPR measurements to detect major discontinuities at Cheshmeh-Shirdoosh limestone quarry, Iran. *Bull. Eng. Geol. Environ.* **2017**, *78*, 743–752. [[CrossRef](#)]
9. Lualdi, M.; Zanzi, L. 2D and 3D experiments to explore the potential benefit of GPR investigations in planning the mining activity of a limestone quarry. In Proceedings of the Tenth International Conference Ground Penetrating Radar, Delft, The Netherlands, 21–24 June 2004.
10. Elkarmoty, M.; Colla, C.; Gabrielli, E.; Bonduà, S.; Bruno, R. A Combination of GPR Survey and Laboratory Rock Tests for Evaluating an Ornamental Stone Deposit in a Quarry Bench. *Procedia Eng.* **2017**, *191*, 999–1007. [[CrossRef](#)]
11. Porsani, J.L.; Sauck, W.A.; Júnior, A.O.S. GPR for mapping fractures and as a guide for the extraction of ornamental granite from a quarry: A case study from southern Brazil. *J. Appl. Geophys.* **2006**, *58*, 177–187. [[CrossRef](#)]
12. Elkarmoty, M.; Bonduà, S.; Bruno, R. A 3D optimization algorithm for sustainable cutting of slabs from ornamental stone blocks. *Resour. Policy* **2020**, *65*, 101533. [[CrossRef](#)]
13. Şirin, E.; Bonduà, S.; Elkarmoty, M. Environmental and economic optimization for block cutting of dimension stones in a limestone quarry. *Resour. Policy* **2021**, *74*, 102396. [[CrossRef](#)]
14. Arriba, M.F.; Díaz-Fernández, M.E.; González-Nicieza, C.; Álvarez-Fernández, M.I.; Álvarez-Vigil, A.E. A computational algorithm for rock cutting optimisation from primary blocks. *Comput. Geotech.* **2013**, *50*, 29–40. [[CrossRef](#)]
15. Ülker, E.; Turanboy, A. Maximum volume cuboids for arbitrarily shaped in-situ rock blocks as determined by discontinuity analysis—A genetic algorithm approach. *Comput. Geosci.* **2009**, *35*, 1470–1480. [[CrossRef](#)]
16. Turanboy, A. A geometric approach for natural rock blocks in engineering structures. *Comput. Geosci.* **2010**, *14*, 565–577. [[CrossRef](#)]
17. Turanboy, A.; Ülker, E. LIP-RM: An attempt at 3D visualization of in situ rock mass structures. *Comput. Geosci.* **2008**, *12*, 181–192. [[CrossRef](#)]
18. Ghozzi, R.; Lahouar, S.; Besbes, K.; Souani, C. Mapping of sewer lines using GPR: A case study in Tunisia. *Data* **2018**, *3*, 40. [[CrossRef](#)]
19. Zhang, J.-X.; Zhang, N.; Xu, Y.-S. Data on point cloud scanning and ground radar of composite lining in jointly constructed tunnel. *Data Brief* **2022**, *41*, 107993. [[CrossRef](#)] [[PubMed](#)]
20. Oualid, M. Electric resistivity data sets for Geohazards subsurface characterization in Guerrara area, southwestern Algeria. *Data Brief* 2018. [[CrossRef](#)]
21. Campana, S.; Piro, S. *Seeing the Unseen: Geophysics and Landscape Archaeology*; CRC Press: Leiden, The Netherlands, 2009; ISBN 978-0-415-44721-8.
22. Conyers, L.B. *Ground-Penetrating Radar for Geoarchaeology*; Wiley-Blackwell Publishers: London, UK, 2016.
23. Conyers, L.B. Medieval Site in Ireland. In *Ground-Penetrating Radar and Magnetometry for Buried Landscape Analysis*; Springer Briefs in Geography; Springer International Publishing: Cham, Switzerland, 2018; pp. 75–90. ISBN 978-3-319-70890-4. [[CrossRef](#)]
24. Gaffney, V.; Patterson, H.; Piro, S.; Goodman, D.; Nishimura, Y. Multimethodological approach to study and characterise Forum Novum (Vescovio Central Italy). *Archaeol. Prospect.* **2004**, *11*, 201–212. [[CrossRef](#)]
25. Goodman, D.; Piro, S. Ground penetrating radar (GPR) surveys at Aiali (Grosseto). In *Seeing the Un-Seen. Geophysics and Landscape Archaeology*; Campana, S., Piro, S., Eds.; Taylor and Francis: London, UK, 2009; pp. 297–302. ISBN 978-0-415-44721-8.
26. Piro, S.; Goodman, D.; Nishimura, Y. The study and characterization of Emperor Traiano’s villa using high-resolution integrated geophysical surveys. *Archaeol. Prospect.* **2003**, *10*, 1–25. [[CrossRef](#)]
27. Radar System Inc. Prism 2 (Version 2.7x) User’s Manual—Riga, LV-1012, Latvia. 2022. Available online: www.radsys.lv (accessed on 1 September 2023).

Disclaimer/Publisher’s Note: The statements, opinions and data contained in all publications are solely those of the individual author(s) and contributor(s) and not of MDPI and/or the editor(s). MDPI and/or the editor(s) disclaim responsibility for any injury to people or property resulting from any ideas, methods, instructions or products referred to in the content.